ELSEVIER

Journal of Organometallic Chemistry 525 (1996) 213–224

Journal of Organometallic Chemistry

Cerium(III) chloride mediated addition of mono- and dilithium ferrocene to (+)-camphor and (−)-fenchone: synthesis and structure of new chiral ferrocenyl alcohols and diols [1]

Vladimir Dimitrov [a,*], Miroslav Genov [a], Svetlana Simova [a,2], Anthony Linden [b,3]

[a] *Institute of Organic Chemistry, Bulgarian Academy of Sciences, BG-1113 Sofia, Bulgaria*
[b] *Organisch-chemisches Institut, Universität Zürich, Winterthurerstrasse 190, CH-8057 Zurich, Switzerland*

Received 1 April 1996

Abstract

Cerium(III) chloride activated (+)-camphor (**1**) and (−)-fenchone (**2**) react with lithiated ferrocene (reagent **3**, $(Li–Cp)_2Fe/LiCp$-FeCp = 50:1) to give the corresponding optically active ferrocenyl diols **4** and **6** and monosubstituted ferrocenyl alcohols **5** and **7**. The preparation of the diols **4** and **6**, as well as of the alcohols **5** and **7** respectively, in high yields is optimized depending on the composition of the lithiated ferrocenes (reagent **3** contains mainly 1,1′-dilithium ferrocene; reagent **8** contains mainly monolithium ferrocene) and on the amounts (stoichiometric, diminished or catalytic) of the $CeCl_3$ used for activation of the ketones **1** and **2**. The catalytic $CeCl_3$ promotion (5 mol%) of the addition reactions of reagents **3** and **8** to **1** and **2** respectively is observed only in the case of fenchone (**2**). The new optically active ferrocenyl alcohols **4**, **5**, **6** and **7** have been studied in detail by NMR, MS and IR spectroscopy. The crystal structure of diol **4** has been determined, and shows an unusual eclipsed conformation of the ferrocenyl moiety, possibly a result of the observed strong intramolecular hydrogen bond formation.

Keywords: Iron; Cerium; Cyclopentadienyl; Chirality; Alcohol; Crystal structure

1. Introduction

Optically active ferrocene derivatives, such as chiral ferrocenylalkylamines [1–4] and ferrocenylphosphines [4] have been utilized as auxiliaries and ligands for a wide range of asymmetric syntheses. Since it has been shown that amino alcohols catalyze the addition of dialkylzinc compounds to aldehydes (for reviews see Ref. [5]), chiral ferrocenyl alcohols have also been synthesized and applied as catalysts [6,7]. To our knowledge, relatively little is known about α-hydroxyalkyl-substituted ferrocene derivatives. Such compounds have been synthesized for the generation of carbonium ions [8] and in the course of investigations on the diastereoselective addition of organomagnesium compounds to 1,1′-diacylferrocenes [9]. Chiral nonracemic ferrocenylalcohols have been produced for the preparation of ferrocenylalkylamines [3] and have been recently synthesized by the enantioselective addition of dialkylzincs to ferrocenecarbaldehyde and ferrocene-1,1′-dicarbaldehyde [10]. Optically active α-hydroxyalkyl ferrocenes are attracting increased interest, because they can be converted into *N,N*-dialkylferrocenylalkylamines with complete retention of the configuration, the latter being highly useful precursors for the synthesis of planar chiral ferrocene derivatives [7,11].

Recently, we have demonstrated that readily available (chiral pool) 1*R*-(+)-camphor (**1**) and 1*R*-(−)-fenchone (**2**) can serve as sources of chiral information in highly diastereoselective syntheses of various chiral alcohols and diols [12–14]. In this paper we present the synthesis of optically active ferrocenyl alcohols and diols using the $CeCl_3$-assisted addition of lithiated ferrocenes to **1** and **2**. Our interest was mainly in the preparation of 1,1′-substituted ferrocenyl diols, since they may possess C_2-symmetry. Such diols are of potential utility for asymmetric synthesis [15]. An exten-

* Corresponding author.
[1] Dedicated to Professor Dr. Herbert Lehmkuhl on the occasion of his 70th birthday.
[2] NMR investigations.
[3] Correspondence concerning crystal structure determination.

PII S0022-328X(96)06498-4

sive amount of structural information for the new ferrocenyl alcohols was obtained from NMR and X-ray crystallographic analyses.

2. Results and discussion

2.1. Remarks on the synthesis and composition of the reagent, 1,1'-dilithium ferrocene

The lithiation of ferrocene with *n*-BuLi in a hexane solution in the presence of TMEDA (*N,N,N',N'*-tetramethylethylenediamine) has been reported to give exclusively 1,1'-dilithium ferrocene as an orange insoluble adduct with TMEDA [16–18]. It has been shown that different amounts of TMEDA might be coordinated with dilithium ferrocene, depending on the excess used during the metallation [18,19].

We prepared 1,1'-dilithium ferrocene according to the published procedure [16] using the molar ratio Cp_2Fe/n-BuLi/TMEDA = 1:2:2, and the resulting reagent was isolated as an orange crystalline solid. In connection with the planned synthesis, it was important to determine the reagent composition. For this purpose the obtained reagent was analysed by ^1H and ^{13}C NMR spectroscopy in THF-d_8 solution, as well as by carbonation with CO_2, followed by isolation of the corresponding 1,1'-disubstituted and monosubstituted acids, whose ratio was then determined by NMR.

For reagent **3**: ^1H NMR (250 MHz, 300 K, THF-d_8): δ = 4.14 ($Cp_{unsubst}$, Li–CpFeCp), 4.00 (α-H–Cp, (Li–Cp)$_2$Fe), 3.68 (β-H–Cp, (Li–Cp)$_2$Fe), 2.29 (CH_2, TMEDA), 2.14 (CH_3, TMEDA). For the Na-salts of 1,1'-ferrocene dicarboxylic acid and ferrocene monocarboxylic acid: ^1H NMR (250 MHz, 300 K, D_2O): δ = 4.64 (α-H–Cp, di-acid), 4.60 (α-H–Cp, mono-acid), 4.37 (β-H–Cp, mono-acid), 4.31 (β-H–Cp, di-acid), 4.20 ($Cp_{unsubst}$, mono-acid).

The data obtained allowed the composition of the reagent to be formulated as (Li–Cp)$_2$Fe/Li–CpFeCp = 50:1, containing approximately one molecule of coordinated TMEDA (reagent **3**). When reproducing the procedure described by Bishop et al. [18] using Cp_2Fe/n-BuLi/TMEDA = 1:2.2:1.2, the obtained ratio of dilithiated-/monolithiated-ferrocene was 30:1.

Reagent **3** with the composition reported above was

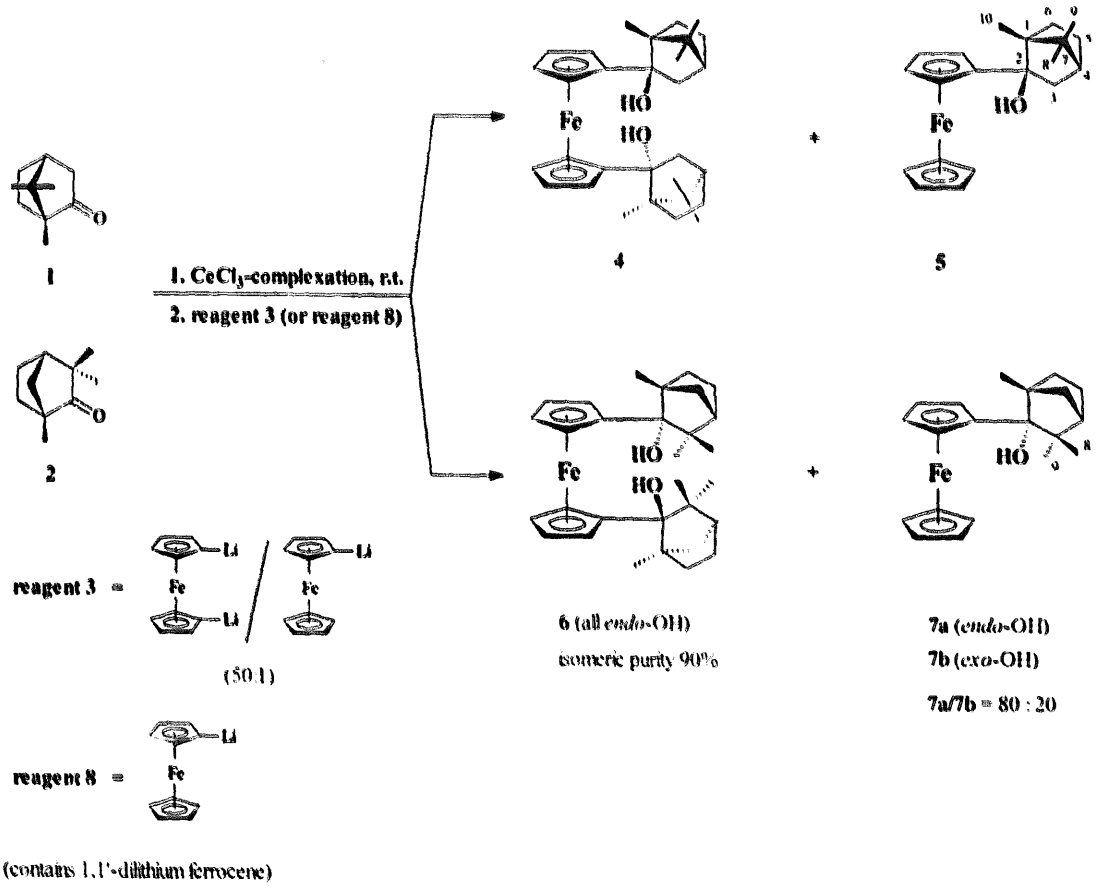

Scheme 1.

Table 1
$CeCl_3$-promoted addition of reagents 3 and 8 to ketones 1 and 2

Entry	Ketone (equiv)	$CeCl_3$ (equiv)	Reagent [a] (equiv)	Conversion of the ketone [b] (%)	Molar ratio diol:alcohol	Yield [c] (%)	
						diol	alcohol
1	1 (1)	1	3 (0.5)	93 [d]	4.4:1	4 (84)	5 (9)
2	1 (1)	0.33	3 (0.5)	66	2.0:1	4 (54)	5 (12)
3	1 (1)	0.10	3 (0.5)	24	0.9:1	4 (16)	5 (8)
4	1 (1)	0.05	3 (0.5)	11	0.4:1	4 (5)	5 (6)
5	2 (1)	1	3 (0.5)	89 [d]	8.7:1	6 (84)	7 (5)
6	2 (1)	0.33	3 (0.5)	89	5.5:1	6 (81)	7 (8)
7	2 (1)	0.10	3 (0.5)	76	4.1:1	6 (68)	7 (8)
8	2 (1)	0.05	3 (0.5)	75	6.4:1	6 (70)	7 (5)
9	1 (1)	1	8	88	1:8.5	4 (17)	5 (71)
10	1 (1)	0.05	8	16	1:4.3	4 (5)	5 (11)
11	2 (1)	1	8	82	1:1.1	6 (53)	7 (29)
12	2 (1)	0.05	8	95	1:8.0	6 (19)	7 (76)

[a] For simplification, reagent 3 was assumed to be $(Li–Cp)_2Fe \cdot TMEDA$; reagent 8 was prepared from ferrocene and ^tBuLi according to Ref. [20], and applied in the ratio ketone/Cp_2Fe/^tBuLi = 1:1.3:1.1.
[b] The conversion is based on the isolated ferrocenyl alcohols.
[c] The products were isolated after column chromatography; yields were calculated with respect to ketones 1 and 2 respectively.
[d] Unreacted ketone was not detected by NMR of the crude products.

used in the experiments described below. For simplification of the stoichiometric calculations, reagent 3 was assumed to be $(Li–Cp)_2Fe \cdot TMEDA$.

2.2. Addition of dilithium ferrocene (reagent 3) to (+)-camphor (1) and (−)-fenchone (2) for the preparation of optically active ferrocenyl diols

The addition of reagent 3 to 1 and 2 respectively, in THF solution, provided, even at room temperature and after several hours, only traces of the mono- and disubstituted addition products (detected by TLC). Ferrocene and unreacted ketones 1 and 2 could be quantitatively isolated after hydrolysis and work up of the reaction mixtures. By applying our procedure [12,14] for activation of 1 and 2 with stoichiometric amounts of anhydrous $CeCl_3$ at room temperature, a quantitative addition of reagent 3 was achieved within 1 h and the resulting diols 4 and 6, respectively, were isolated in high yields [4] (Scheme 1). Surprisingly, significant quantities of the monosubstituted ferrocenyl alcohols 5 and 7 were also obtained. The diols and the mono alcohols were isolated in pure form by column chromatography. The observed ratios 4/5 and 6/7 respectively (Table 1, entries 1 and 5) were quite different from the corresponding ratio of the dilithiated-/monolithiated-ferrocene in reagent 3. This observation indicates that the reaction of the ketones 1 and 2 with the second lithiated centre of the 1,1'-dilithium ferrocene does not proceed completely. Therefore, the dilithiated ferrocene in reagent 3 also serves as a precursor for the monoalcohols 5 and 7.

The application of diminished and catalytic amounts of $CeCl_3$ in order to activate 1 and 2 and to promote the addition of reagent 3 according to our previous observations [12], provided interesting results. The conversion of the ketones, as well as the ratio of the disubstituted-/monosubstituted-ferrocenyl alcohol depended on the $CeCl_3$ quantities used (Table 1 and Fig. 1). In the case of ketone 1, 5 mol% of $CeCl_3$ did not catalyze the addition of reagent 3; poor conversion of the ketone was observed. When the amounts of $CeCl_3$ were increased, the conversion of ketone 1 also increased, being acceptable when stoichiometric quantities of $CeCl_3$ were used. In contrast, 5 mol% of $CeCl_3$ provided very good conversion of ketone 2 during the addition of reagent 3. Increasing the quantities of $CeCl_3$ used for activation of 2 improved the observed conversion relatively little. Surprisingly, the product ratio of the alcohols 4/5 and 6/7, respectively, strongly depends on the mole fraction of $CeCl_3$ used for the activation of the ketones 1 and 2 (Table 1 and Fig. 1). In the case of camphor (1), the observed dependence of the conversion and the 4/5 ratio on the amounts of the $CeCl_3$ can be explained by the nearly absent catalytic activity of the alkoxycerium(III) species, which are formed in situ during the addition reactions [12]. Therefore, for a higher conversion and a higher 4/5 ratio, ketone 1 would need to be activated with stoichiometric quantities of $CeCl_3$ in order to react with reagent 3 and

[4] Different amounts of ferrocene were always isolated after work-up of the reaction mixtures (see Section 3). This indicates that the lithiated ferrocenes in reagent 3 were in a moderate excess with respect to the ketones 1 and 2.

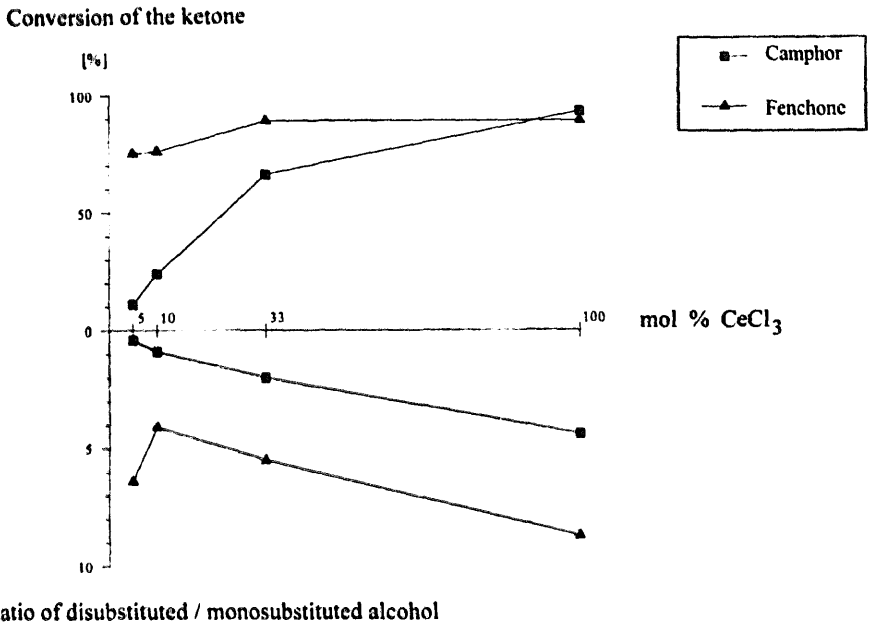

Fig. 1. Graphical presentation of the relationship between the amounts of $CeCl_3$ used in the addition reactions of reagent **3** and the conversion of the ketones **1** and **2**, as well as the ratio of disubstituted/monosubstituted ferrocenyl alcohols.

especially with the second lithium function of the dilithiated ferrocene. An analogous trend was observed with the ketone **2** for the **6/7** ratio when 10, 33 and 100 mol% of $CeCl_3$ were used. The high **6/7** ratio in favour of diol **6** in the case of 5 mol% (Fig. 1 and Table 1, Entry 8) should be noted as remarkable. It is difficult to discuss the results presented in Fig. 1 because any explanation would need to take account of the role of the different kinds of alkoxycerium(III) species formed in situ, which would be speculative.

As expected [12–14], the stereoselectivity of the addition reactions was connected with an *endo*-attack of reagent **3** to **1** and, preferably, an *exo*-attack in the case of ketone **2**. These results allowed the definition of the absolute configuration of the newly formed chiral centre at the C-2 position as 2*S* for the camphor-derived alcohols and as 2*R* for the fenchone-derived alcohols (Scheme 1). For the monosubstituted fenchone derivative a diastereoisomeric ratio **7a/7b** = 80:20 was detected by NMR experiments. In the case of the diol **6** (all *endo*-OH, isomeric purity 90%), the presence of diastereoisomeric products (*endo/exo* isomers) was detected by NMR, but could not be determined quantitatively.

Table 2
Properties and analytical data for compounds **4**–**7**

Compound	M.p. (°C)	$[\alpha]_D^{20}$ ($CHCl_3$)	IR (cm^{-1})				Elemental analyses
			ν [a]	0.001 M (CCl_4)	0.05 M (CCl_4)	KBr	
4	198 (decomp.)	+1.33 (*c* 0.75)	ν_1	3620 w	3620 vw	3620 s	$C_{10}H_{42}O_2Fe$ (490.5)
			ν_2	3548 m	3548 vw		calc.: C, 73.43; H, 8.63
			ν_3	3450 s	3456 w	3413 s	found: C, 73.31; H, 8.75
5	119–120	−72.18 (*c* 0.76)	ν_2	3548 m	3548 m	3556 m	$C_{20}H_{26}OFe$ (338.3) calc.: C, 71.01; H, 7.75 found: C, 70.91; H, 7.41
6	134–135	−82.72 (*c* 0.77)	ν_1	3613 w	3613 vw	3613 w	$C_{10}H_{42}O_2Fe$ (490.5)
			ν_2	3548 m	3548 w	3548 m	calc.: C, 73.43; H, 8.63
			ν_3	3480 s	3480 w	3480 w	found: C, 73.52; H, 8.51
7	80–83	−48.87 (*c* 0.71)	ν_2	3543 m	3543 m	3530 m	$C_{20}H_{26}OFe$ (338.3) calc.: C, 71.01; H, 7.75 found: C, 70.89; H, 7.80

[a] νOH: ν_1 free OH group; ν_2 OH · · · d-electrons hydrogen bond; ν_3 OH · · · O intramolecular hydrogen bond.

The ferrocenyl alcohols **4–7** are yellow crystalline solids with defined melting points (for physical data, see Section 3, Table 2). They are readily soluble in $CHCl_3$ and CH_2Cl_2 and have relatively low solubility in hydrocarbons. The diol **4** is nearly insoluble in pentane and hexane, which could be used for its isolation in a pure form from **4–5**-mixtures.

2.3. Addition of monolithium ferrocene (reagent 8) to (+)-camphor (1) and (−)-fenchone (2)

For the synthesis of the monosubstituted alcohols **5** and **7** in good yields, the preparation of monolithium ferrocene was necessary. The direct monolithiation of ferrocene with *n*-BuLi provided unsatisfactory results [21]. It has been reported recently by Kagan and coworkers [20] that the metallation of ferrocene with ^tBuLi in THF affords monolithium ferrocene in a 70% yield. Reproducing this procedure, we prepared monolithium ferrocene (reagent **8**) and allowed it to react with the $CeCl_3$ (stoichiometric) activated ketones **1** and **2** (Table 1, entries 9 and 11). The conversion of the ketones was high in both cases; however, the formation of the diols **4** and **6** in large quantities was also observed. Therefore, reagent **8** contained significant amounts of dilithium ferrocene, whose content was not separately determined. The use of equimolar quantities of $CeCl_3$ provided, after the addition of **8** to ketone **1**, the alcohol **5** in good yield (71%, entry 9). In contrast, in the case of ketone **2**, formation of the diol **6** was favoured (entry 11). The addition of reagent **8** to **1**, activated with 5 mol% $CeCl_3$ (entry 10), had no practical utility, since the conversion was low. In contrast, ketone **2** reacted quantitatively with **8** when activated with 5 mol% $CeCl_3$ and the monosubstituted alcohol **7** was formed as the main product (entry 12). These results were somewhat surprising; however, their discussion would again require a better knowledge of the role of the alkoxycerium(III) species formed in situ. These species appear to be acting as catalysts for the addition reactions [12]. The variation of the $CeCl_3$ quantities permitted the optimization of the synthesis of the monosubstituted alcohols **5** and **7** in order to maximize the yields.

2.4. Molecular structure of 1,1'-bis{(1R,2S)-2-exo-hydroxy-1,7,7-trimethylbicyclo[2.2.1]hept-2-yl}ferrocene (4)

A view of the molecule of **4** showing the atom numbering scheme is presented in Fig. 2. Selected interatomic distances and angles are listed in Table 3. The absolute configuration of the molecule was determined crystallographically (see Section 3) and confirmed that the ligands have the 1*R*,2*S* configuration. The Cp-rings lie parallel to one another with all Fe–C

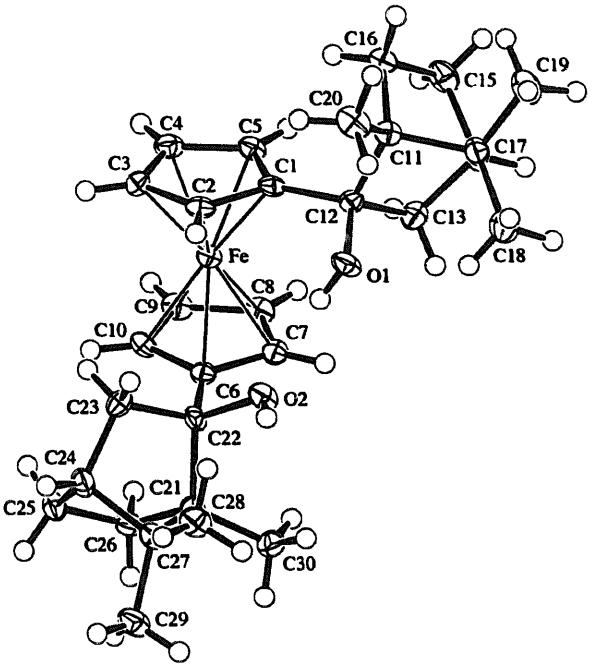

Fig. 2. An ORTEP drawing of the molecular structure of **4** (50% probability ellipsoids; arbitrary spheres for the H-atoms).

Table 3
Selected interatomic distances (Å) and bond angles (deg) for **4**

Fe–C(1)	2.059(3)	C(11)–C(16)	1.545(4)
Fe–C(2)	2.052(3)	C(11)–C(17)	1.572(4)
Fe–C(3)	2.050(3)	C(12)–C(13)	1.557(4)
Fe–C(4)	2.045(3)	C(13)–C(14)	1.542(4)
Fe–C(5)	2.034(3)	C(14)–C(15)	1.534(4)
Fe–C(6)	2.061(3)	C(14)–C(17)	1.549(5)
Fe–C(7)	2.055(3)	C(15)–C(16)	1.555(4)
Fe–C(8)	2.057(3)	C(21)–C(22)	1.576(4)
Fe–C(9)	2.044(3)	C(21)–C(26)	1.539(4)
Fe–C(10)	2.038(3)	C(21)–C(27)	1.576(4)
O(1)–C(12)	1.437(3)	C(22)–C(23)	1.554(4)
O(2)–C(22)	1.445(3)	C(23)–C(24)	1.542(4)
C(1)–C(12)	1.523(4)	C(24)–C(25)	1.539(4)
C(6)–C(22)	1.515(4)	C(24)–C(27)	1.551(4)
C(11)–C(12)	1.570(4)	C(25)–C(26)	1.544(4)

C(2)–C(1)–C(12)	125.0(3)	C(11)–C(16)–C(15)	103.8(2)
C(5)–C(1)–C(12)	128.3(3)	C(11)–C(17)–C(14)	92.7(2)
C(7)–C(6)–C(22)	125.0(3)	C(22)–C(21)–C(26)	106.9(2)
C(10)–C(6)–C(22)	128.2(3)	C(22)–C(21)–C(27)	102.4(2)
C(12)–C(11)–C(16)	107.4(2)	C(26)–C(21)–C(27)	100.6(2)
C(12)–C(11)–C(17)	103.0(2)	O(2)–C(22)–C(6)	103.2(2)
C(16)–C(11)–C(17)	100.9(2)	O(2)–C(22)–C(21)	111.0(2)
O(1)–C(12)–C(1)	108.1(2)	O(2)–C(22)–C(23)	112.4(2)
O(1)–C(12)–C(11)	106.4(2)	C(6)–C(22)–C(21)	114.3(2)
O(1)–C(12)–C(13)	112.1(2)	C(6)–C(22)–C(23)	114.5(2)
C(1)–C(12)–C(11)	115.3(2)	C(21)–C(22)–C(23)	101.7(2)
C(1)–C(12)–C(13)	113.2(3)	C(22)–C(23)–C(24)	104.8(2)
C(11)–C(12)–C(13)	101.4(2)	C(23)–C(24)–C(25)	107.2(3)
C(12)–C(13)–C(14)	104.6(2)	C(23)–C(24)–C(27)	102.3(2)
C(13)–C(14)–C(15)	107.3(2)	C(25)–C(24)–C(27)	102.6(3)
C(13)–C(14)–C(17)	102.6(3)	C(24)–C(25)–C(26)	102.5(2)
C(15)–C(14)–C(17)	102.9(3)	C(21)–C(26)–C(25)	104.7(2)
C(14)–C(15)–C(16)	102.6(2)	C(21)–C(27)–C(24)	93.1(2)

Table 4
^{1}H NMR data for the ferrocenyl alcohols **4–7**, *endo*-methyl borneol [12] and *exo*-methyl fenchol [12] (solvent $CDCl_3$, δ (ppm) relative to TMS); assignments marked with asterisks are tentative; for the numbering of the C-atoms, see Schemes 1 and 2

Compound	3-H$_{exo}$ 7-H$_{syn}$	3-H$_{endo}$ 7-H$_{anti}$	4-H	5-H$_{exo}$	5-H$_{endo}$	6-H$_{exo}$	6-H$_{endo}$	8-H	9-H	10-H	2′-H	3′-H	4′-H	5′-H	Cp	OH
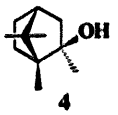	2.06	1.36	1.71	1.67	1.02	1.36	1.34	1.10	0.86	0.84	—	—	—	—	1.24 CH_3	n.o.
4	2.29	1.88	1.78	1.67	1.08	1.15	1.08	1.22	0.87	0.75	4.27	4.20	4.14	4.17	—	3.13
5	2.25	1.85	1.77	1.65	0.99 *	1.15	1.03 *	1.22	0.86	0.79	4.24	4.17	4.17	4.17	4.20	2.59
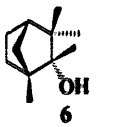	1.56	1.00	1.64	1.44	1.72	0.99	1.89	0.95	0.93	0.99	—	—	—	—	1.10 CH_3	n.o.
6	1.85	1.10	1.61	1.30	1.69	1.12	2.18	0.41	0.96	1.42	4.17	4.00	4.26	3.96	—	2.87
7a	1.82	1.11	1.62	1.35	1.73	1.07	2.32	0.46	0.95	1.42	4.14	4.12	4.27	4.06	4.17	2.14
7b	2.14	1.04	1.60	1.36	1.54	1.32	1.86	1.05	0.54	1.40	4.33	4.21	4.21	4.17	4.21	2.79

bonds being equivalent. The angle between the planes of the two Cp-rings is only 2.5° and the rings adopt the gauche eclipsed conformation with the overlapping C-atoms almost perfectly eclipsed. There is a strong intramolecular hydrogen bond between the hydroxy group of one ligand, O–1H, and the hydroxy group of the second ligand (H(11) ··· O(2) = 1.99(3), O(1) ··· O(2) = 2.786(3) Å; O(1)–H(11) ··· O(2) = 162(3)°). The second hydroxy group does not act as a hydrogen bond donor for additional hydrogen bonds. It is likely that the intramolecular hydrogen bond helps to stabilize the eclipsed conformation of the Cp-rings. That the same conformation is retained in solution (see below) may also be due to this strong hydrogen bond.

2.5. Determination of the structure and solution conformation of 4–7 by NMR and IR spectroscopy

The unambiguous assignments of the ^{1}H and ^{13}C NMR spectra of **4–7**, achieved by homonuclear (double quantum filtered COSY) and heteronuclear (standard and inverse H–C) correlation experiments, confirm the

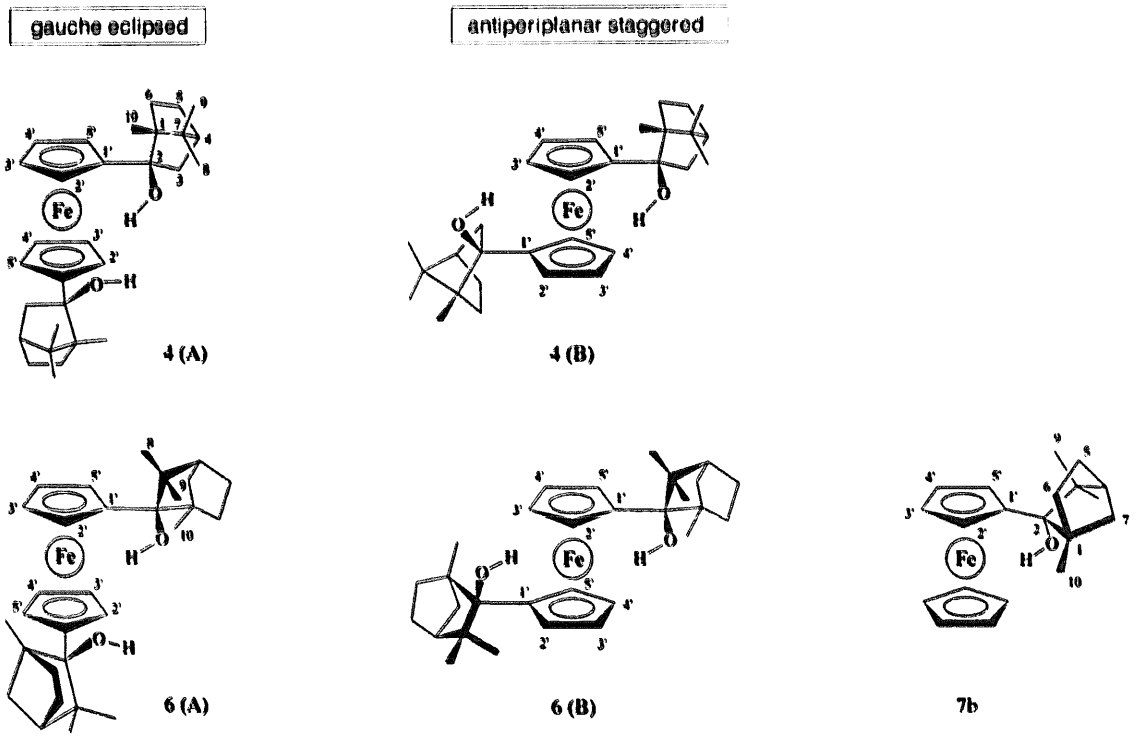

Scheme 2.

Table 5
^{13}C NMR data for the ferrocenyl alcohols 4–7 (solvent $CDCl_3$, δ (ppm) relative to TMS); assignments marked with asterisks are tentative; for the numbering of the C-atoms, see Schemes 1 and 2

Compound	C-1	C-2	C-3	C-4	C-5	C-6	C-7	C-8	C-9	C-10	C-1'	C-2'	C-3'	C-4'	C-5'	Cp
4	52.81	80.93	47.46	45.60	26.89	31.56	50.00	21.57	21.57	9.91	96.17	67.80	68.09	67.39	68.31	—
5	52.41	80.34	47.09	45.66	26.83	31.65	49.97	21.46	21.31	9.88	97.11	66.31	68.74 *	67.71 *	68.38 *	68.15
6	52.39	81.28	45.39	49.49	25.05	31.98	41.06	29.55	21.94	19.27	95.79	68.84	67.02	68.01	69.31	—
7a	52.42	80.43	44.60	49.69	25.29	31.83	40.90	29.76	22.02	19.36	96.58	66.54	66.08	67.73	69.96	68.55
7b	52.91	80.59	45.55	48.10	26.70	30.25	42.64	25.82	26.85	18.74	96.67	69.23	67.70 *	66.46 *	67.17	68.55

expected constitution of the compounds (Tables 4 and 5). Distance constraints, obtained by NOE difference spectroscopy (see Section 3) allow: (i) the establishment of the absolute configuration of the newly formed chiral centres at C-2 (*exo*- or *endo*-OH) in the bicyclic part of the molecules, for which no crystal structure is available; (ii) the determination of the solution conformations of the compounds by also using the observed Cp-ring current-induced proton chemical shifts. The solution conformation is dependent on the disposition of the bicyclic moiety with respect to the attached Cp-ring, as well as on the torsional twist around the Cp–Fe–Cp axis in the case of the diols **4** and **6**. Two major conformers have been observed: gauche eclipsed **A** and antiperiplanar staggered **B** (Scheme 2).

2.5.1. *Camphor-derived ferrocenyl alcohols 4 and 5*

The 2*S* absolute configuration (*endo*-Cp substitution), taking into account the known 1*R* configuration for **4** and **5**, results from the observed nuclear Overhauser enhancements between the hydroxy protons and the closely spaced C-8 methyl and 3-H_{exo} protons. The NOE determined proton proximities show that the predominant solution conformer of **4** retains its solid-state structure, i.e. gauche eclipsed **A** (Scheme 2). One of the α-H–Cp protons, the 2'-H, lies close to the C-10 methyl and the hydroxy group, whereas the other, 5'-H, is near the 3-H_{endo} and 6-H_{endo} protons. Both the 3-H_{endo} and 3-H_{exo} protons fall into the deshielding region of the second Cp-ring. This can be demonstrated by comparison with the chemical shifts of the corresponding protons in *endo*-methyl borneol (Table 4). The observed NOE between 3-H_{exo} and 2'-H further confirms the eclipsed conformation of **4** and is the result of an interaction with the 2'-H from the other Cp-ring. However, there are weak NOEs between the hydroxy group and 3'-H, 4'-H and 5'-H, obviously protons from the other Cp-ring, which is possible only when the antiperiplanar staggered conformation is present. The IR data (see below) also support the occurrence of conformation **B** in solution. The NMR data for compounds **4** and **5** are similar, indicating that their structures and conformations in solution are identical — the disposition of the bicyclic moiety with respect to its attached Cp-ring for **4** and **5** is the same. Analogously to **4**, the unsubstituted Cp-ring in **5** is located nearest to the C-3 atom.

2.5.2. *Fenchone-derived ferrocenyl alcohols 6 and 7*

The NMR investigations of the alcohols **6** and **7** have been carried out on samples which were *endo*/*exo*-mixtures of isomers (Scheme 1, Tables 4 and 5). The diastereoisomeric purity of **6** was 90% as determined from proton NMR intensities. The minor isomers of **6** (all-*exo*-OH, 2*S* configuration or mixed *endo*/*exo*-OH, 2*R*/2*S* configuration) could not be characterized due to severe overlapping. For the monoalcohol **7**, a ratio of **7a**/**7b** = 80:20 was determined. The proton chemical shifts of the minor isomer **7b** (Table 4) have been resolved from the inverse C–H correlation experiment. Both main isomers of **6** and **7** showed quite similar NMR data. The preferred disposition of the bicyclic moiety with respect to the connected Cp-ring could be determined from the observed NOEs of the α-H–Cp-protons. The proton denoted as 2'-H lies close to the C-8 methyl protons, whereas 5'-H is close to the 7-H_{syn} and 10-H protons. The *exo*-Cp-substitution in the major isomers of **6** and **7** could also be deduced from the strong deshielding of the C-8 methyl carbons, similar to previous observations [14]. The other Cp-ring lies opposite to the C-3 carbon atom and near the C-10 methyl group, due to the steric hindrance of the C-8 and C-9 methyl groups. The C-10 methyl protons are deshielded by approximately 0.4 ppm (Cp-ring current effect) compared with the corresponding *exo*-methyl-fenchol (Table 4).

The NOE data for the diol **6** indicate that, besides the hydrogen bond stabilized gauche eclipsed **A** conformer, a conformer with antiperiplanar staggered Cp-rings **B** is present in solution, both being approximately equally populated. The latter conformation is indicated by the proximity of the C-10 methyl and the hydroxy protons to 4'-H and 3'-H from the distant Cp-ring respectively.

Although the minor isomer **7b** (*endo*-Cp-substitution, 2*S* configuration) could not be isolated in pure form, some structural data were obtained. The proton denoted as 2'-H is pointing to the 6-H_{endo} and close to the C-10 methyl protons (Scheme 2). When compared with **4** and **5**, the bicyclic moiety is rotated about the C–1'–C-2

bond, most probably due to the steric hindrance between the C-9 methyl group and the substituted Cp-ring. The distant Cp-ring is near the C-10 methyl group and opposite to the C-3 carbon atom, as in isomer **7a**.

2.5.3. IR data for the ferrocenyl alcohols 4–7

The IR spectra of the diols **4** and **6** showed three OH bands, whereas the monoalcohols exhibited only one (Table 2). For compounds **4** and **6**, in addition to the strong intramolecular OH · · · O hydrogen bond, another absorption at 3548 cm^{-1} occurs. This band corresponds to an OH · · · d hydrogen bond resulting from the interaction of the hydroxy protons with d-electrons from the iron atom. The absorption of the free hydroxy group at low concentrations is weak. The observed data are in accordance with previously published results [22]. We can explain these observations by the existence of both conformers **A** and **B** in solutions of the diols **4** and **6** — OH · · · O hydrogen bonds and free OH for the gauche eclipsed conformation, and OH · · · d interactions for the antiperiplanar staggered conformation. The conformation deduced from the IR spectrum of solid **4** (KBr) corresponds to that found in the X-ray structure (conformation **A**) — an OH · · · O hydrogen bond and a free hydroxy group were observed. In contrast, for the diol **6**, an OH · · · d absorption is present, indicating that this compound exists in the solid state in both conformations **A** and **B** (Scheme 2). In the case of the monoalcohols **5** and **7**, only OH · · · d absorptions were observed, indicating that the interaction of the hydroxy protons with the d-electrons of the iron atom plays a significant role.

3. Experimental section

3.1. General

All reactions were carried out in flame-dried Schlenk flasks under an argon atmosphere. THF was distilled over Na–benzophenone. Pentane and hexane were distilled over $Na[Et_4Al]$. Anhydrous $CeCl_3$ was prepared according to the literature procedure [12]. The organolithium compounds *n*-BuLi (1.33 M in hexane) [23] and ^{t}BuLi (0.72 M in pentane) [20] were prepared according to literature procedures. Thin layer chromatography (TLC): aluminium sheets precoated with silica gel 60 (0.063–0.200 mm, Merck). Melting points: Kofler-block apparatus (uncorrected). $[\alpha]_D^{20}$: Perkin–Elmer 241 polarimeter. IR spectra: Specord 75 IR Carl Zeis Jena. Mass spectra (MS): Jeol-JMS-D-300 spectrometer; fragment ions in *m/z* with relative intensities (%) in parentheses. NMR spectra: Bruker Avance DRX-250 (^{1}H at 250.1 MHz; ^{13}C at 62.9 MHz; TMS as internal standard). The samples for the NOE experiments were prepared under inert conditions, using $CDCl_3$ dried (molecular sieve 4 Å) and distilled under argon; several irradiations were performed in one experiment with automatic cycling through frequency lists for each multiplet (the individual lines in the multiplet were irradiated for 0.1 s, the whole irradiation time was 5 s) and for the off-resonance position; 32 scans with two dummy scans for each frequency list were acquired and then the experiment was repeated 20 times. To the difference between the on- and off-resonance irradiation free induction decay, a line broadening of 0.5 Hz was applied before FT. The irradiation power was adjusted to suppress approximately 80% of the multiplet intensity. Elemental analyses were performed by the Microanalytical Service Laboratory of the Institute of Organic Chemistry (Sofia).

3.2. Preparation of 1,1'-dilithium ferrocene (reagent 3)

To a stirred mixture from 21.80 g (117.20 mmol) Cp_2Fe in 400 ml hexane was added dropwise an *n*-BuLi · TMEDA solution in hexane, prepared from 176 ml (234.08 mmol) 1.33 M *n*-BuLi–hexane and 27.20 g (234.08 mmol) TMEDA. During the addition of *n*-BuLi · TMEDA, a dark red-orange solution was formed, from which, after 2–3 h, the crystallization of the metallated ferrocene began. After stirring for 24 h, the solid was filtered, washed with hexane (2 × 40 ml) and dried in vacuo to give 28.44 g (77% yield related to Cp_2Fe) of reagent **3** as an orange pyrophoric solid.

3.3. Preparation of 1,1'-bis[(1R,2S)-2-exo-hydroxy-1,7,7-trimethylbicyclo[2.2.1]hept-2-yl]ferrocene (4)

A mixture of 1.21 g (4.91 mmol) $CeCl_3$ and 0.75 g (4.93 mmol) (1*R*-(+)-camphor in 10 ml THF was stirred for 40 min at room temperature, during which a slightly yellow gel-like mixture was formed. The ferrocenyllithium reagent **3** (0.77 g, 2.45 mmol) was added rapidly in solid form at room temperature during which the heterogeneous mixture turned to a deep red-orange solution and the temperature increased to ca. 40 °C. After 1 h stirring at room temperature the mixture was hydrolysed with 2 N HCl, extracted with CH_2Cl_2 (3 × 30 ml) and the organic layer was dried over $MgSO_4$. The crystalline residue remaining after evaporation of the solvent (contains Cp_2Fe, **4** and **5**) was extracted with ca. 35 ml pentane, to give after filtration 0.89 g of pure **4**. After evaporation of the pentane filtrate, the residue was chromatographed (*h* = 430 mm, Ø 13 mm, 22 g silica gel 60, 0.063–0.200 mm, hexane/Et_2O = 30:1) to give 0.06 g ferrocene, 0.16 g (9%) of **5** and 0.12 g of **4**. The total yield of **4** (yellow crystals) was 1.01 g (84%).

Data for **4**: MS (70 eV): *m/z* = 490 (M^+, 100), 472 ($M^+ - H_2O$, 80), 454($M^+ - 2H_2O$, 20), 272 (40), 254 (30). IR (KBr) cm^{-1}: 3620 s, 3413 s, 2940 m, 2860 w, 1470 s, 1450 m, 1380 s, 1360 m, 1340 w, 1290 w, 1110 s, 1054 s, 1001 m, 960 m, 900 w, 840 m, 800 m, 510 m, 490 m.

Data for **5**: MS (70eV): $m/z = 338$ (M^+, 100), 255 (20). IR (KBr) cm^{-1}: 3556m, 2900m, 2860m, 1450m, 1380m, 1360m, 1340w, 1290w, 1110s, 1060s, 1030w, 1020w, 1000m, 960m, 810s, 490m.

Observed NOEs ($CDCl_3$, 300K); s (strong), m (medium) and w (weak) correspond to effects of greater than 7%, 2–7% and less than 2% respectively:

Irradiated proton	Compound **4**	Compound **5**
3_{exo}	3_{endo} (s), 4 (m), 8 (m), OH (m), 2′ (m)	3_{endo} (s), 4 (m), 8 (m), OH (w)
3_{endo}	3_{exo} (s), 5_{endo} (w), 5′ (s)	3_{exo} (s), 5_{endo} (w), 5′ (s)
5_{endo}, 6_{endo}	3_{endo} (s), 4 (m) 5_{exo} (m), 5′ (s)	3_{endo} (m), 4 (s), 5_{exo} (s), 5′ (s)
10	6 (m), 2′ (s)	6 (m), 8 (w), OH (w), 2′ (s)
OH	3_{exo} (w), 8 (m), 2′ (s), 3′ (w), 4′ (w), 5′ (w)	3_{exo} (w), 8 (w), 2′ (m), $Cp_{unsubst}$ (m)
2′	3_{exo} (w), 10 (m), OH (s)	10 (w), OH (m)
5′	3_{endo} (s), 3_{exo} (w), 6_{endo} (m)	3_{endo} (m), 6_{endo} (m)

3.4. Preparation of 1,1′-bis{(1R,2R)-2-endo-hydroxy-1,3,3-trimethylbicyclo[2.2.1]hept-2-yl}ferrocene (6)

A mixture of 1.82g (7.38mmol) $CeCl_3$ and 1.12g (7.36mmol) (1*R*)-(−)-fenchone in 12ml THF was stirred for 40min at room temperature, during which a yellow gel-like mixture was formed. The ferrocenyllithium reagent **3** (1.16g, 3.69mmol) was added rapidly in solid form at room temperature in the course of which the heterogeneous mixture turned to a deep red-orange solution and the temperature increased to ca. 40°C. After stirring for 1h at room temperature the mixture was hydrolysed with 2N HCl and extracted with Et_2O (3 × 40ml). The organic layer was washed with 5% $NaHCO_3$ (10ml) then with water (3 × 30ml) and dried over $MgSO_4$. The residue remaining after evaporation of the solvent was chromatographed (*h* = 520mm, Ø24mm, 88g silica gel 60, 0.063–0.200mm, hexane/Et_2O = 30:1) to give 0.11g ferrocene, 0.12g (5%) of **7** and 1.52g (84%) of **6**.

Data for **6**: MS (70eV): $m/z = 490$ (M^+, 95), 472 ($M^+ - H_2O$, 100), 444 (22). IR (KBr) cm^{-1}: 3613w, 3548m, 3480w, 2920s, 2850m, 1450s, 1370m, 1360m, 1300m, 1250w, 1110m, 1050s, 1020w, 1000m, 980m, 900w, 870m, 840s, 650w, 580w, 540w, 520m, 490s.

Data for **7**: MS (70eV): $m/z = 338$ (M^+, 100), 213 (100) 186 (Cp_2Fe, 65), 121 ($CpFe^+$, 35). IR (KBr) cm^{-1}: 3530m, 2920s, 2850m, 1450s, 1400w, 1370m, 1360m, 1300m, 1250w, 1100s, 1050s, 1030m, 1020m, 980s, 900w, 870m, 810s, 650w, 580w, 520m, 490s.

Observed NOEs ($CDCl_3$, 300K); s (strong), m (medium) and w (weak) correspond to effects of greater than 7%, 2–7% and less than 2% respectively:

Irradiated proton	Compound **6**	Compound **7a**	Compound **7b**
6_{endo}	5_{endo} (s), 6_{exo} (s), OH (m)	5_{endo} (w), 6_{exo} (s)	2′ (m)
7_{syn}	4 (m), 7_{anti} (s), 8 (m), 5′ (s)	4 (w), 7_{anti} (s), 8 (w), 5′ (m)	
8	4 (s), 7_{syn} (s), 9 (m), 2′ (m) 3′ (w), 4′ (w), 5′ (w)	4 (s), 7_{syn} (m), 2′ (s)	4 (m)
9	5_{endo} (s), 8 (m), OH (m), 2′ (m)	5_{endo} (s), 4 (m), 8 (s), 2′ (m)	4 (s), 8 (m) 5_{endo} (m)
10	2′ (s), 3′ (s), 4′ (w), 5′ (s)	6_{exo} (s), 5′ (s), $Cp_{unsubst}$ (s)	OH (s), 2′ (s) $Cp_{unsubst}$ (s)
OH	6_{endo} (m), 8 (w), 9 (m), 2′ (s) 3′ (m), 4′ (w), 5′ (w)	10 (w), 5′ (m) $Cp_{unsubst}$ (m)	$Cp_{unsubst}$ (s)
2′	8 (w), 9 (w), 10 (m), OH (m) 3′ (m)	8 (w), 9 (w), OH (w)	
3′	10 (m), 2′ (m), 4′ (m)	n.o.	
5′	7_{syn} (m), 7_{anti} (w indirect) 10 (s), 4′ (m)	7_{syn} (m), 10 (m), 4′ (m)	
Cp		10 (w), OH (w)	OH (w)

3.5. Preparation of 1-{(1R,2S)-2-exo-hydroxy-1,7,7-trimethylbicyclo[2.2.1]hept-2-yl}ferrocene (5)

For the preparation of monolithium ferrocene (reagent **8**), 4 ml (2.88 mmol) ^{t}BuLi in pentane were added to a stirred mixture of 0.65 g (3.49 mmol) Cp_2Fe in 5 ml THF at 0°C. After stirring for 30 min at 0°C, the mixture was warmed to room temperature and was applied as reagent **8**. To a mixture of 0.65 g (2.64 mmol) $CeCl_3$ and 0.40 g (2.63 mmol) (1*R*-(+)-camphor in 8 ml THF, stirred for 40 min at room temperature, reagent **8** was added, during which the heterogeneous mixture turned to a deep red-orange solution. After stirring for 1.5 h, the reaction mixture was hydrolysed with 2 N HCl, extracted with CH_2Cl_2 (3 × 30 ml) and dried ($MgSO_4$). The residue remaining after evaporation of the solvent was chromatographed (h = 520 mm, Ø 24 mm, 87 g silica gel 60, 0.040–0.063 mm, hexane/Et_2O = 30:1) to give 0.65 g ferrocene, 0.63 g (71%) of **5** and 0.11 g (17%) of **4**.

3.6. Preparation of 1-{(1R,2R)-2-endo-hydroxy-1,3,3-trimethylbicyclo[2.2.1]hept-2-yl}ferrocene (7)

For the preparation of monolithium ferrocene (reagent **8**), 3.9 ml (2.81 mmol) ^{t}BuLi in pentane were added to a stirred mixture of 0.62 g (3.33 mmol) Cp_2Fe in 5 ml THF at 0°C. After stirring for 30 min at 0°C, the mixture was warmed to room temperature and was applied as reagent **8**. To a mixture of 0.032 g (0.130 mmol) $CeCl_3$ and 0.39 g (2.56 mmol) (1*R*)-(−)-fenchone in 8 ml THF, stirred for 40 min at room temperature, reagent **8** was added, during which a deep red-orange solution was formed. After stirring for 1.5 h, the reaction mixture was hydrolysed with 2 N HCl, extracted with CH_2Cl_2 (3 × 30 ml) and dried ($MgSO_4$). The residue remaining after evaporation of the solvent was chromatographed (h = 520 mm, Ø 24 mm, 87 g silica gel 60, 0.040–0.063 mm, hexane/Et_2O = 30:1) to give 0.28 g ferrocene, 0.66 g (76%) of **7** and 0.12 g (19%) of **6**.

3.7. X-ray structure determination for 1,1'-bis{(1R,2S)-2-exo-hydroxy-1,7,7-trimethylbicyclo[2.2.1]hept-2-yl}-ferrocene (4)

All measurements were made on a Rigaku AFC5R diffractometer using graphite-monochromated Mo Kα radiation (λ = 0.71069 Å) and a 12 kW rotating anode generator. The intensities of three standard reflections were measured after every 150 reflections and remained stable throughout the data collection. The intensities were corrected for Lorentz and polarization effects. Azimuthal scans of several reflections and the minimum and maximum transmission factors from a trial numerical absorption correction indicated that an absorption correction was unnecessary. The data collection included the measurement of the Friedel opposites of all unique reflections with $2\theta < 40°$. Equivalent reflections, other than Friedel pairs, were merged. The data collection and refinement parameters are given in Table 6.

The structure was solved by Patterson methods using SHELXS86 [24], which revealed the position of the Fe-atom. All remaining non-hydrogen atoms were located in a Fourier expansion of the Patterson solution. The non-hydrogen atoms were refined anisotropically. The H-atoms of the hydroxy groups were placed in the positions indicated by a difference electron density map and their positions were allowed to refine together with individual isotropic temperature factors. All of the remaining H-atoms were fixed in geometrically calculated positions (d(C–H) = 0.95 Å) with fixed isotropic temperature factors assigned to be $1.2U_{eq}$ of the parent C-atom. The orientations of the methyl group H-atoms were based on peaks located in a difference electron density map. Refinement of the structure was carried out on F using full-matrix least squares procedures, which minimized the function $\Sigma w(|F_o| - |F_c|)^2$. The weighting scheme was based on counting statistics and included a factor to downweight the intense reflections.

Table 6
Crystallographic data for **4**

Crystallised from	chloroform–pentane
Empirical formula	$C_{30}H_{42}FeO_2$
Formula weight	490.51
Crystal colour, habit	orange-yellow, prism
Crystal dimensions (mm)	0.23 × 0.25 × 0.43
Temperature (K)	173(1)
Crystal system	orthorhombic
Space group	$P2_12_12_1$
Z	4
Reflections for cell determination	23
2θ range for cell determination (deg)	35–40
a (Å)	15.168(3)
b (Å)	22.717(3)
c (Å)	7.200(2)
V (Å^3)	2481.1(8)
F(000)	1056
D_x (g cm^{-3})	1.313
μ(Mo Kα) (mm^{-1})	0.632
Scan type	$\omega/2\theta$
$2\theta_{(max)}$ (deg)	55
Total reflections measured	5704
Symmetry independent reflections	4453
R_{merge}	0.083
Reflections used ($I > 2\sigma(I)$)	3983
Parameters refined	307
R	0.0389
R_w	0.0360
Weighting scheme	$1/w = \sigma^2(F_o) + (0.005F_o)^2$
Goodness of fit	1.740
Secondary extinction coefficient	$1.40(5) \times 10^{-6}$
Final Δ_{max}/σ	0.0003
$\Delta\rho$(max; min) (e Å^{-3})	0.41; −0.56

Table 7
Fractional atomic coordinates and equivalent isotropic temperature factors for 4

Atom	x	y	z	U_{eq} [a] (Å^2)
Fe	0.13640(3)	0.80068(2)	0.12963(6)	0.0166(1)
O(1)	0.0406(1)	0.89957(9)	0.4677(3)	0.0249(7)
O(2)	0.2214(2)	0.9100(1)	0.4073(3)	0.0234(7)
C(1)	0.0253(2)	0.8108(1)	0.2906(4)	0.0171(8)
C(2)	0.0930(2)	0.7820(1)	0.3931(4)	0.0191(8)
C(3)	0.1174(2)	0.7294(1)	0.2998(4)	0.0215(9)
C(4)	0.0640(2)	0.7248(1)	0.1375(5)	0.0230(9)
C(5)	0.0079(2)	0.7751(1)	0.1315(5)	0.0197(8)
C(6)	0.2470(2)	0.8532(1)	0.1452(5)	0.0185(8)
C(7)	0.1788(2)	0.8824(1)	0.0456(4)	0.0194(9)
C(8)	0.1549(2)	0.8477(1)	−0.1113(4)	0.0221(9)
C(9)	0.2089(2)	0.7963(1)	−0.1093(4)	0.0232(9)
C(10)	0.2650(2)	0.7997(1)	0.0479(4)	0.0200(8)
C(11)	−0.1079(2)	0.8622(1)	0.4543(4)	0.0193(9)
C(12)	−0.0185(2)	0.8685(1)	0.3464(5)	0.0179(9)
C(13)	−0.0470(2)	0.9066(1)	0.1770(5)	0.025(1)
C(14)	−0.1466(2)	0.9169(1)	0.2055(4)	0.026(1)
C(15)	−0.1932(2)	0.8582(1)	0.1674(5)	0.028(1)
C(16)	−0.1676(2)	0.8207(1)	0.3399(5)	0.0228(9)
C(17)	−0.1542(2)	0.9231(1)	0.4191(4)	0.025(1)
C(18)	−0.1075(2)	0.9783(1)	0.4964(6)	0.040(1)
C(19)	−0.2493(2)	0.9255(2)	0.4895(6)	0.037(1)
C(20)	−0.0967(2)	0.8438(1)	0.6556(5)	0.028(1)
C(21)	0.3743(2)	0.9158(1)	0.2830(4)	0.0181(8)
C(22)	0.2906(2)	0.8764(1)	0.3197(4)	0.0175(9)
C(23)	0.3287(2)	0.8280(1)	0.4495(4)	0.0210(9)
C(24)	0.4270(2)	0.8439(1)	0.4715(5)	0.0229(9)
C(25)	0.4724(2)	0.8306(1)	0.2850(5)	0.024(1)
C(26)	0.4367(2)	0.8799(1)	0.1581(5)	0.0221(9)
C(27)	0.4247(2)	0.9121(1)	0.4741(4)	0.0213(9)
C(28)	0.3788(2)	0.9377(1)	0.6494(5)	0.028(1)
C(29)	0.5166(2)	0.9410(1)	0.4664(5)	0.029(1)
C(30)	0.3533(2)	0.9769(1)	0.2065(4)	0.026(1)

[a] U_{eq} is defined as one-third of the trace of the orthogonalized U_{ij} tensor.

Plots of $\sum w(|F_o| - |F_c|)^2$ vs. $|F_o|$), reflection order in data collection, $\sin\theta/\lambda$ and various classes of indices showed no unusual trends. A correction for secondary extinction was applied.

Neutral atom scattering factors for non-hydrogen atoms were taken from Maslen et al. [25], and the scattering factors for H-atoms were taken from Stewart et al. [26]. Anomalous dispersion effects were included in F_{calc} [27]; the values for f' and f'' were those of Creagh and McAuley [28]. All calculations were performed using the TEXSAN crystallographic software package [29].

The absolute configuration was determined by performing an additional refinement of the completed structure together with the enantiopole, or Flack's x, parameter [30] using the program CRYSTALS [31]. This parameter converged to −0.03(2), which confidently confirms that the refined coordinates, as listed in Table 7, represent the true enantiomorph.

Complete tables of atomic coordinates, bond lengths and angles have been deposited with the Cambridge Crystallographic Data Centre. Lists of observed and calculated structure factors and of thermal displacement parameters are available from the authors.

Acknowledgements

Support of this work by the Bulgarian National Fund for Scientific Research is gratefully acknowledged.

References

[1] R. Hermann, G. Hübener, F. Siglmüller and I. Ugi, *Justus Liebigs Ann. Chem.*, (1986) 251.
[2] F. Siglmüller, R. Hermann and I. Ugi, *Justus Liebigs Ann. Chem.*, (1989) 623.
[3] I. Ugi, D. Marquarding and R. Urban, in B. Weinstein, (ed.), *Chemistry and Biochemistry of Aminoacids, Peptides and Proteins*, Vol. VI, Marcel Dekker, New York, 1982.
[4] T. Hayashi, in A. Togni and T. Hayashi (eds.), *Ferrocenes: Homogeneous Catalysis, Organic Synthesis, Material Science*, Weinheim, New York, (VCH, Tokyo) 1995, p. 105.
[5] (a) R. Noyori, S. Suga, K. Kawai, S. Okada and M. Kitamura, *Pure Appl. Chem.*, *60* (1988) 1597. (b) R. Noyori and M. Kitamura, *Angew. Chem.*,*103* (1991) 34. (c) K. Soai and S. Niwa, *Chem. Rew.*, *92* (1992) 833.
[6] (a) M. Watanabe, S. Araki, Y. Butsugan and M. Uemura, *J. Org. Chem.*, *56* (1991) 2218. (b) M. Watanabe, N. Hashimoto, S. Araki and Y. Butsugan, *J. Org. Chem.*, *57* (1992) 742.
[7] Y. Butsugan, S. Araki and M. Watanabe, in A. Togni and T. Hayashi (eds.), *Ferrocenes: Homogeneous Catalysis, Organic Synthesis, Material Science*, Weinheim, New York, (VCH, Tokyo) 1995, p. 143.
[8] (a) M.J.A. Habib and W.E. Watts, *J. Chem. Soc. C*, (1969) 1469. (b) M.J.A. Habib and W.E. Watts, *J. Chem. Soc. C*, (1970) 2552. T.D. Turbitt and W.E. Watts, *J. Chem. Soc. Perkin II*, (1974) 177. (d) T.D. Turbitt and W.E. Watts, *J. Chem. Soc. Perkin II*, (1974) 185. (e) S. Braun, T.S. Abram and W.E. Watts, *J. Organomet. Chem.*, *97* (1975) 429. (f) K. Yamakawa and M. Hisatome, *J. Organomet. Chem.*, *52* (1973) 407. (g) G.H. Williams, D.D. Traficante and D. Seyferth, *J. Organomet. Chem.*, *60* (1973) C53. (h) Y. Okada and T. Hayashi, *Magn. Reson. Chem.*, *30* (1992) 892.
[9] P. Canone, G. Foscolos and R. Harder, *J. Organomet. Chem.*, *178* (1979) 331.
[10] K. Soai, T. Hayase, K. Tokai and T. Sugiyama, *J. Org. Chem.*, *59* (1994) 7908 and references cited therein.
[11] Y. Matsumoto, A. Ohno, S. Lu, T. Hayashi, N. Oguni and M. Hayashi, *Tetrahedron: Asymmetry*, *4* (1993) 1763 and references cited therein.
[12] V. Dimitrov, S. Bratovanov, S. Simova and K. Kostova, *Tetrahedron Lett.*, *35* (1994) 6713.
[13] V. Dimitrov, K. Kostova and M. Hesse, *Tetrahedron: Asymmetry*, *5* (1994) 1891.
[14] V. Dimitrov, S. Simova and K. Kostova, *Tetrahedron*, *52* (1996) 1699.
[15] (a) C. Rosini, L. Francini, A. Raffaelli and P. Salvadori, *Synthesis*, (1992), 503. (b) J.K. Whitesell, *Chem. Rev.*, *89* (1989) 1581. (c) D. Seebach, D.A. Plattner, A.K. Beck, Y.M. Wang and D. Hunziker, *Helv. Chim. Acta*, *75* (1992) 2171. (d) D. Seebach, R. Dahinden, R.E. Marti, A.K. Beck, D.A. Plattner and F.N.M. Kühnle, *J. Org. Chem.*, *60* (1995) 1788.
[16] M.D. Raush and D.J. Ciappenelli, *J. Organomet. Chem.*, *10* (1967) 127.

[17] M.D. Raush, G.A. Moser and C.F. Naede, *J. Organomet. Chem.*, *51* (1973) 1.
[18] J.J. Bishop, A. Davison, M.L. Katcher, D.W. Lichtenberg, R.E. Merrill and J.C. Smart, *J. Organomet. Chem.*, *27* (1971) 241.
[19] M. Herberhold, in A. Togni and T. Hayashi (eds.), *Ferrocenes: Homogeneous Catalysis, Organic Synthesis, Material Science*, Weinheim, New York, (VCH, Tokyo) 1995, p. 223 and relevant literature cited therein.
[20] F. Rebiere, O. Samuel and H.B. Kagan, *Tetrahedron Lett.*, *31* (1990) 3121.
[21] S.I. Goldberg, L.H. Keith and T.S. Prokopov, *J. Org. Chem.*, *28* (1963) 850.
[22] P. Canonne, G. Foscolos and R. Harder, *J.Organomet. Chem.*, *178* (1979) 331.
[23] U. Schöllkopf in E. Müller (ed.), *Houben–Weyl Methoden der Organischen Chemie*, Vol. XIII/1, Georg Thieme, 1970, p. 136.
[24] G.M. Sheldrick, SHELXS-86, *Acta Crystallogr. Sect. A:*, *46* (1990) 467.
[25] E.N. Maslen, A.G. Fox and M.A. O'Keefe, in A.J.C. Wilson (ed.), *International Tables for Crystallography*, Vol. C, Kluwer Academic, Dordrecht, 1992, Table 6.1.1.1, pp. 477–486.
[26] R.F. Stewart, E.R. Davidson and W.T. Simpson, *J. Chem. Phys.*, *42* (1965) 3175.
[27] J.A. Ibers and W.C. Hamilton, *Acta Crystallogr.*, *17* (1964) 781.
[28] D.C. Creagh and W.J. McAuley, in A.J.C. Wilson (ed.), *International Tables for Crystallography*, Vol. C, Kluwer Academic, Dordrecht, 1992, Table 4.2.6.8, pp. 219–222.
[29] TEXSAN, *Single Crystal Structure Analysis Software*, Version 5.0, Molecular Structure Corporation, The Woodlands, TX, 1989.
[30] (a) H.D. Flack, *Acta Crystallogr. Sect. A:*, *39* (1983) 876. (b) G. Bernardinelli and H.D. Flack, *Acta Crystallogr. Sect. A:*, *41* (1985) 500.
[31] D.J. Watkin, J.R. Carruthers and P.W. Betteridge, CRYSTALS *User Guide*, Chemical Crystallography Laboratory, Oxford, UK, 1985.